Casimir repulsion beyond the dipole regime

Alexander P. McCauley,[1] Alejandro W. Rodriguez,[2, 3] M. T. Homer Reid,[1, 4] and Steven G. Johnson[3]

[1]*Department of Physics, Massachusetts Institute of Technology, Cambridge, MA 02139, USA*
[2]*School of Engineering and Applied Sciences, Harvard University, Cambridge, MA 02139, USA*
[3]*Department of Mathematics, Massachusetts Institute of Technology, Cambridge, MA 02139, USA*
[4]*Research Laboratory of Electronics, Massachusetts Institute of Technology, Cambridge, MA 02139, USA*

We extend a previous result [Phys. Rev. Lett. 105, 090403 (2010)] on Casimir repulsion between a plate with a hole and a cylinder centered above it to geometries in which the central object can no longer be treated as a point dipole. We show through numerical calculations that as the distance between the plate and central object decreases, there is an intermediate regime in which the repulsive force increases dramatically. Beyond this, the force rapidly switches over to attraction as the separation decreases further to zero, in line with the proximity force approximation. We demonstrate that this effect can be understood as a competition between an increased repulsion due to a larger polarizability of the central object interacting with increased fringing fields near the edge of the plate, and attractive forces due primarily to the nonzero thickness of the plate. In comparison with our previous work, we find that using the same plate geometry but replacing the single cylinder with a ring of cylinders, or more generally an extended uniaxial conductor, the repulsive force can be enhanced by a factor of approximately 10^3. We conclude that this enhancement, although quite dramatic, is still too small to yield detectable repulsive Casimir forces.

I. INTRODUCTION

Although Casimir forces (a generalization of van der Waals forces to macroscopic objects) between neutral metal objects in vacuum are normally attractive interactions [2, 3], in our previous work we showed that the force can become repulsive for objects of certain shapes, and in particular we showed that repulsion occurred for a needle-like particle above a metal plate with a hole [Fig. 1 (a)] for which an analytical symmetry argument applied [1]. In this work, we address two questions: first, is repulsion limited to systems where one particle is very small or can it be obtained for two objects of length scales comparable to their separation; and second, is this repulsion necessarily weak (10 aN for a single particle in Ref. 1) or can it theoretically be made stronger in comparison with other Casimir forces without simply shrinking the entire system (for perfect conductors, multiplying all dimensions by a scale factor a changes the force by a factor of $1/a^2$, but in actual systems there is a limit to the minimum achievable length scales). In answer to these questions, we find that a thousand-fold enhancement of the repulsion is theoretically possible without changing the hole radius or overall length scales. This is accomplished by replacing the original needle-like particle of Fig. 1(a) (in this case a circular cylinder of high aspect ratio) with a macroscopic array of identical particles [Fig. 1(b)], effectively forming a capsule of uniaxial conducting material [Fig. 1(c)]. To understand the mechanism behind this enhancement, we separately consider the repulsion as a single cylinder is displaced off-axis as well as the screening interaction when multiple cylinders are combined. For a single cylinder we find that there is an optimal off-axis position where the repulsion is enhanced (up to 50 times) due to the presence of strong fringing fields. The presence of this optimal position is a consequence of the competing repulsive and attractive

effects of fringing fields and proximity-force approximation (PFA) [4] interactions, respectively. As the cylinder is brought closer to the plate, the PFA forces take over and the repulsion vanishes. The Casimir force is non-additive, and the total force between the array of cylinders and the plate will not simply be a sum of the forces between the individual cylinders and the plate. However, we find that the non-additive contributions (or screening effects) associated with the presence of multiple cylinders are surprisingly small: the enhancement does not saturate until there are dozens of cylinders with separation significantly smaller than the cylinder length. We furthermore find that this repulsion persists when realistic conductivities are included, and when the capsule is anchored to a substrate by via a long oxide post. Although substantial experimental challenges remain in fabricating this particular structure, these results, combined with previous work on effective uniaxial/anisotropic media [5–10] suggests that strongly anisotropic metamaterials offer new opportunities to achieve exotic Casimir interactions.

To begin with, we review the argument of Ref. 1 that describes repulsion in the dipole regime. Consider the setup of Fig. 1 (a), consisting of a thin plate with a hole of radius R and a thin cylinder with center a distance z above the hole and oriented normal to the plate. Assume that the cylinder is exactly centered on the hole, so that by cylindrical symmetry the total force is parallel to the z axis. In the limit that this cylinder is infinitesimal, only dipolar charge/current fluctuations on the cylinder are allowed, and the energy is given by the Casimir-Polder energy of a point dipole across from the hole. If the plate is perfectly conducting but has zero thickness $T = 0$ [27], a repulsive force follows from a symmetry argument: when the needle is at $z = 0$, dipolar symmetry prevents charge fluctuations of the needle from coupling to the plate and vice versa. The Casimir-Polder energy at $z = 0$ must therefore be zero. As $z \to \infty$ (fixing
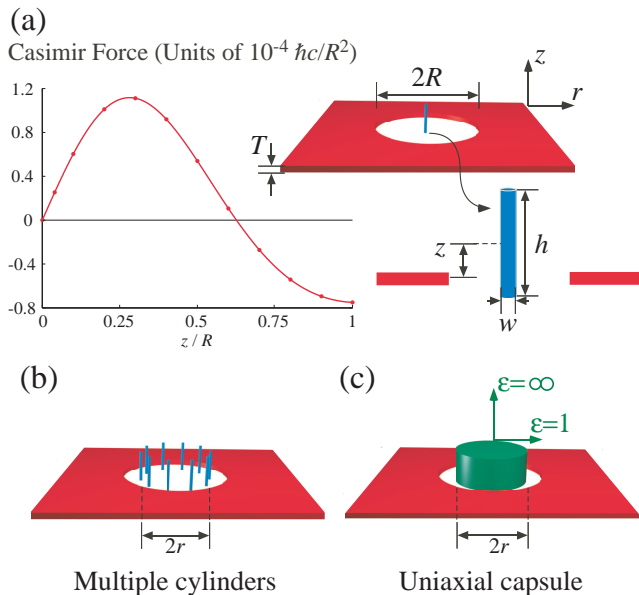
FIG. 1: Configurations used in the text. *Top*: Reference configuration, from Ref. 1. *Top Left*: Geometry illustrating the single plate-needle configuration. *Top Right*: Casimir force vs. vertical height z for the configuration in the top left panel. Positive forces denote repulsion. *Bottom*: The two generalizations considered here: *Bottom Left*: Replacing a single cylinder with a ring of N (in the figure, $N = 10$) cylinders, each of which is more closely spaced to the edge of the hole. *Bottom Right*: An idealized version of the cylinder ring configuration, consisting of a cylinder of uniaxial conductance in the vertical (z) direction.

$\mathbf{x} = 0$), the (Casimir-Polder) energy must be negative, as in this limit the geometry is equivalent to a needle and a uniform plate. Therefore, at some point the derivative of the energy with respect to z must be negative, implying a net repulsive force. This argument is rigorously true for an infinitesimal needle centered at $\mathbf{x} = 0$ across from a perfectly thin plate. When the needle is of finite size $h > 0$, but still of a high aspect ratio $h \gg w$ (e.g., a long cylinder, so as to be primarily polarizable in the z-axis), and the plate is of finite thickness but with $R \gg T$, we found in Ref. 1 that the repulsive force persists as long as $h \lesssim R/2$.

This repulsive force is interesting in that it can neither be interpreted as arising (qualitatively) from pairwise-additive forces [11–15] or from an effective-medium interpretation [7, 16–19] (for other such exceptions, see Ref. 3). However, as found in Ref. 1, the magnitude of this repulsive force is extremely small (on the order of 10 aN for the geometry considered in that work), due to both the smallness of the needle and its large distance ($R \sim 500\,\text{nm}$) from the edge of the plate. Therefore, aside from examining the repulsive effect beyond the dipole regime, another motivation of this work is to examine how greatly the repulsive force can be enhanced. An obvious way to increase the absolute magnitude of the force would be to shrink all dimensions of the sys-

tem uniformly by a scaling factor a—for perfect conductors, the force will scale as $1/a^2$ by dimensional analysis. However, for real materials there is a lower limit to the dimensions that can be achieved before material effects (e.g., the skin depth for gold) become important. For the present case, the most important geometric parameter is the thickness T of the plate, which must be nonzero for any physical configuration—we expect that T should be larger than the skin depth of gold in order for our analysis to be valid. As discussed in Ref. 1, the repulsive effect requires $T/R \ll 1$; setting, e.g., $T \sim 20\,\text{nm}$ as in Ref. 1 as an optimistic lower bound on a real plate thickness constrains the minimal value for R, and hence the overall force magnitude.

The basic principle of repulsion in this system lies in the charge fluctuations of the plane decoupling from fluctuations of the needle at $z = 0$. Then when considering more general geometries we should have in mind a cylindrically-symmetric object of conductivity primarily along the z-axis, which is our motivation for considering the configurations of Fig. 1 (c,d). In both cases, due to the close contact between the center object and the edge of the plate, it is essential to account for finite-size effects, making analytic or semi-analytic calculation difficult. Furthermore, in the presence of a thick plate we cannot rely on a general symmetry argument to guarantee repulsion for any range of parameters. As a result, the results of this work are entirely numerical. The two computational tools we use for our analysis are a boundary-element method (BEM) [20] and a finite-difference time-domain (FDTD) method [21, 22], both of which involve the adaptation of numerical techniques from classical electromagnetism for Casimir force computation. For simplicity, we primarily assume perfectly-conducting materials, and we further drop the requirement of a separating plane between the two objects (while still requiring that the cylindrical object be more than halfway out of the plane, so that the "repulsion" is not due to a trivial redefinition of coordinates). Additionally, to make a fair definition of "enhancement", we work within geometric constraints for the plate similar to Ref. 1. One last fact bears mentioning before proceeding further: in the cylindrically symmetric case, the net Casimir force is along the z-axis. However, this force is intrinsically unstable [23]: a small radial displacement of any of the configurations of Fig. 1 off the z-axis will result in a large, attractive radial component to the Casimir force. Therefore, to prevent this translational instability any configuration must be confined in the radial direction by, e.g., external mechanical forces.

II. ENHANCEMENT OF FRINGING FIELDS

As noted in [1], the repulsive forces arise from fringing fields due to the sharp edges around the hole of the plate; this holds for both perfectly thin ($T = 0$) and thicker plates. Drawing on our intuition from electrostatics, for
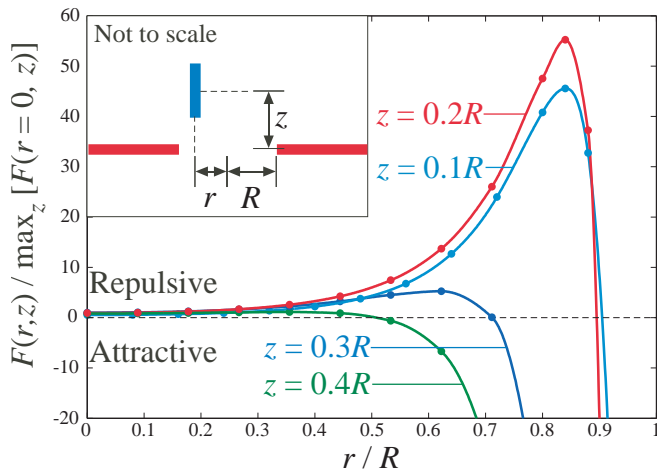
FIG. 2: The effect of fringing fields on F_z, the z-component of the Casimir force for a single metallic cylinder: for a fixed z, F_z is enhanced as r increases. Plotted above is F_z for several values of z/R, normalized by the maximum of the repulsive force $(0.0278\,\hbar c/R^2)$ for $x = 0$. As $r \to R$, F_z undergoes a very strong enhancement, peaking at approximately 55 for $r \sim 0.8R$ and $z = 0.2R$. For every z, as x increases pairwise attractive forces take over and F_z switches sign (note that for $r \neq 0$ there is an attractive force F_x between the cylinder and the plate edge, so the total Casimir force is not strictly repulsive in this case). Shown for reference in the inset is F_z (in units of $\hbar c/R^2$) at $r = 0$.

any fixed plate geometry we suspect that these fields are greatly enhanced as the plate edges are approached (i.e., $r = |\mathbf{r}| > 0$). If the plate thickness is *a priori* fixed, it is possible that this enhancement of the fringing fields leads to an enhanced repulsive effect for some range of r. Because the repulsive force is unstable in the transverse direction, a single cylinder displaced by $r > 0$ will experience a strong (attractive) radial force; to compensate for this, we would need to include, e.g., multiple cylinders displaced symmetrically about $r = 0$ to make the net radial force zero. However, to understand the effects of the fringing fields alone it is more illuminating to first consider the z-component $F_z(r, z)$ of the Casimir force, as a function of r and z, between a *single* cylinder at position (r, z) and a *thin* ($T = 0$) plate, as depicted in Fig. 2 (Inset). For definiteness, the cylinder is taken to have height $h = 0.64R$ and width $w = 0.04R$ (the same units as in Ref. 1). In this case, the plate is taken to be a circular annulus of inner radius R and outer radius $8R$, the latter being large enough to eliminate finite-size effects on the force.

The results, computed with BEM, are shown in Fig. 2, where all dimensions are given in units of R. As our goal is to examine the force relative to the $r = 0$ case, we normalize the force results by the peak repulsive force along the z-axis, i.e., $F(r, z)/\max_z[F(r = 0, z)]$. Moving away from $r = 0$, we find that this ratio is consistently larger than 1 for all z plotted. This increase can be quite large (up to 55 times larger) before the force rapidly switches

sign to attraction. We propose the following explanation for this effect: as $r \to R$, the fringing fields of the thin plate, which are induced by dipolar charge/current fluctuations of the cylinder, grow without bound. This leads to an enhanced plate-dipole coupling with increasing r, which for fixed z should lead to an enhanced repulsion if the force at that z is repulsive for $r = 0$. However, when the cylinder-plate separation becomes comparable to the cylinder height h, higher-order (i.e., non-dipolar) currents on the cylinder will begin to contribute to the energy. As these higher-order multipole currents are not bound by the dipolar symmetry argument of Ref. 1, we expect their contribution to the force to be attractive in general. With this interpretation, the force curves of Fig. 2 show a competition between the contribution of dipole currents on the cylinder, which is repulsive for certain z and grows without bound as $r \to R$, and the contributions of higher-order cylinder currents which are attractive and grow more rapidly than the dipole term as $r \to R$.

This argument is supported by the results of Fig. 2, and raises a further interesting theoretical question: is it possible to *increase* the repulsive effect by *decreasing* the size of the cylinder (while keeping its aspect ratio constant)? The motivation for this is that a smaller cylinder can be brought closer to the edge of the plate before higher order currents contribute (attractively) to the force, therefore taking greater advantage of the increased fringing fields and leading to a larger repulsive net force. (Note that this does not violate PFA, because whenever we have repulsion we are assuming h is always comparable to the surface-surface separation.) Numerical computations (see below) support this argument; however, a rigorous analysis is of course required to confirm this. As this is of course an unphysical limit, we will not perform such an analysis here. Rather, we simply use this observation to illustrate that it is crucial to account for the finite thickness T of the plate: once $R - r \sim T$, a cylinder of any size will induce higher-order currents on the plate, which will also lead to attraction. A non-zero value of T must therefore be set in order to obtain physically meaningful force bounds.

We now consider the more realistic case of the force between a cylinder an a finite thickness ($T > 0$) plate in Fig. 3. In light of the argument presented above, we also study the effect for several values of h. On a technical note, use of the boundary-element method requires that the size of the mesh used to discretize the surfaces be smaller than any characteristic separation. However, now that $T > 0$, we must place two copies of the annulus used above within a distance T of each other. As $T \ll R$, this requires a much denser mesh than used above in the thin plate case. Roughly, the number of surface mesh elements will scale as T^{-2}, so that the overall spatial and temporal resource requirements scale as $\sim T^{-4}$ and $\sim T^{-6}$, respectively [20]. Due to this rather steep scaling, we find that for the range of T considered here an annulus with outer radius of $8R$ proves too computationally demanding. To

FIG. 4: Enhancement of Casimir repulsion with a a realistic geometry (Fig. 1, Bottom Left): in place of a single cylinder, a ring of N cylinders is placed at radius r (shown for $N = 5$ in the inset). The cylinders have height $h/R = 0.64$, and for computational tractability the plate thickness T is zero. For small N the force increases linearly, with slope corresponding approximately to the magnitude of enhancement of Fig. 2. As N increases, the effect saturates. As in previous figures, the force is maximized over z.
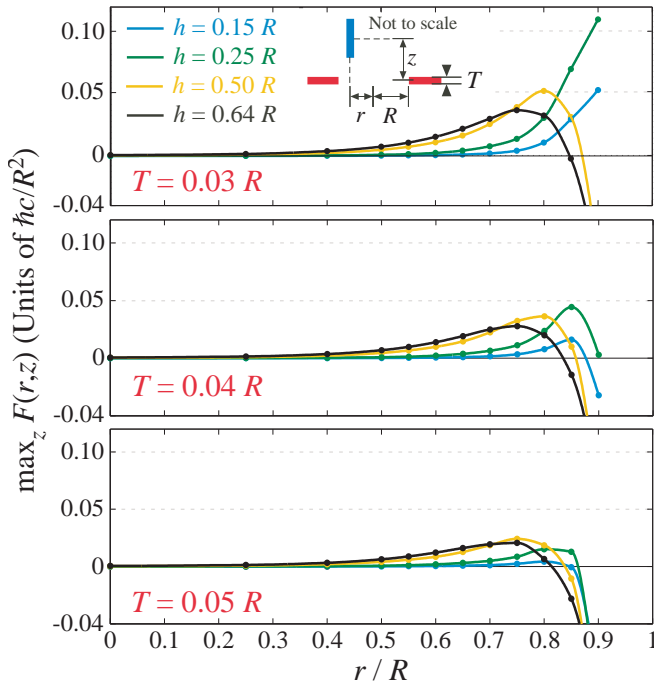
FIG. 3: The effect of plate thickness on the Casimir force on a single cylinder. For each panel, the plate thickness is fixed and the Casimir force (maximized over $z > 0$) on a single cylinder is plotted as a function of x. The force for different values of cylinder height h are shown (for each h, the aspect ratio of the cylinder is fixed). For small T (Top), decreasing the cylinder size can actually lead to an increased repulsion for $x \sim R$. Increasing T (Middle and Bottom) leads to a decreased repulsion for all cylinders at all x, but the effect is strongest for small h cylinders.

reduce the overall number of surface mesh elements, we truncate the outer radius at $1.6R$ instead; although there will now be finite-size effects, we estimate their effect at well below 10% of the total force in all cases. We examine three plate thicknesses $T/R = 0.03, 0.04, 0.05$ and five different values of h/R. For each cylinder value of h, the corresponding cylinder width is chosen to as to keep a constant cylinder aspect ratio. The results are shown in Fig. 3; to simplify the presentation, for each T we plot only the maximum repulsive force force $\max_{z>0} F_z(r, z)$ for each r. The top panel of Fig. 3 supports the argument given in the previous paragraph: although for most values of r, $h = 0.64R$ gives the largest repulsive force, as $r/R \to 1$, cylinders of progressively smaller size exhibit a stronger repulsion. (Although we expect that the limits $h \to 0$, $r/R \to 1$ and $T \to 0$ can be taken in such a way as to make the peak repulsion unbounded, numerical limitations make computation of forces with $r/R > 0.9$ difficult.) On the other hand, as T increases the attractive contributions of higher-order plate currents turn on at progressively smaller r. Further, this effect is strongest for the small-h cylinders, as shown by successive panels of Fig. 3. For example, by $T/R = 0.04$ the force curves
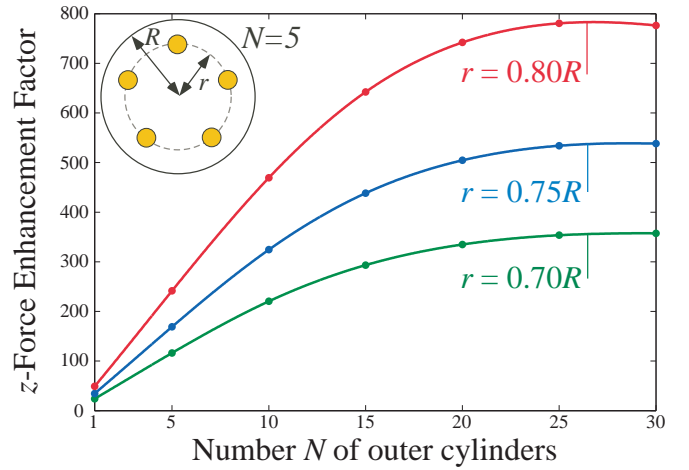
for $h < 0.25R$ now show attraction by $r = 0.9R$, and for $T/R = 0.05$, the cylinders with $h/R \sim 0.5$ now show the strongest repulsive effect when maximized over all r. In contrast to the strong T-dependence of the force for small h, for $h = 0.64R$ the results are quantitatively altered (approximately 50%), but the order of magnitude of the repulsive effect remains. On the basis of this, we conclude that for the range of thicknesses we are interested in, the best value of h/R is in the range $h/R \sim 0.5$.

III. MULTIPLE CYLINDERS AND UNIAXIAL CAPSULES

Previously, we found that the repulsive force is greatly enhanced as a cylinder is brought close to the edge of a plate—how close depended on both the cylinder height h and the plate thickness T. It is reasonable to assume that this effect should be enhanced if multiple cylinders are now added, bearing aside non-additive cylinder-cylinder interactions. In particular, if N cylinders are spread about a ring of radius r, one expects that for N not too large the repulsive force should scale linearly with N. As N increases, cylinder-cylinder interactions will take over. In Sec. III A, we will examine this behavior in detail. We find that the non-additive cylinder-cylinder interactions simply lead to a saturation of the repulsive effect, and that the value of N at which this occurs is quite high, leading to a large force enhancement. In the limit of large N, it is appropriate to replace the ring of cylinders with a homogeneous cylindrical capsule of uniaxial conductivity Fig. 1(d). This is examined in Sec. III B,

and allows us to obtain an upper bound for the repulsive force in our system. In addition, as these systems have rotational symmetry, the net force is along the z-axis and there is no longer an attractive radial component.

A.   Multiple cylinders

We examine the effect of multiple cylinders with BEM simulations. Due to the computational limitations in BEM for a plate of finite thickness, we cannot directly simulate multiple cylinders next to a thick plate. Instead, we utilize the fact (see Fig. 3) that a cylinder of $h = 0.64R$ is not strongly affected by a finite but small slab thickness and perform BEM simulations for a thin plate instead. We expect that these results will still be approximately valid for plate thicknesses $T \lesssim 0.05R$. The results of these computations are shown in Fig. 4 for three values of ring radius r/R. For small N, the z-force increases approximately linearly, with the slope roughly corresponding to the size of the enhancement factor for a single cylinder in Fig. 2 (red curve) for the value $x \sim r$. As N increases, non-additive cylinder-cylinder interactions become important, and this linear enhancement eventually saturates. However, it is interesting that this saturation does not occur until fairly large N, at which point the peak enhancement factor is ~ 800 for $r = 0.8R$ (larger r exhibit weaker repulsion, in line with Fig. 2). Further, it is interesting to observe that increasing N past this saturation point does not have an appreciable effect on the force: the additional cylinders are simply screened, and net repulsive force is practically unchanged. Additional calculations (not shown) for thinner cylinders show very similar values for the peak repulsion, with saturation after this peak. This leads us to believe that the ideal uniaxial capsules, shown in Fig. 1 (d), are actually a fairly good approximation to the more realistic configuration of many cylinders considered here. The advantage of the uniaxial capsules, examined in the next section, is that we can easily simulate them in FDTD and incorporate the thick plate, which as stated before is crucial for obtaining a realistic bound on the repulsion.

B.   Uniaxial capsules

The basic mechanism of the repulsive effect relies on combining fringing fields with objects of high, anisotropic conductivity. Until this point, this anisotropy has been realized via the shape of the objects. However, as argued in the previous section, the limit in which the cylinders are allowed to become arbitrarily narrow and densely packed is well-defined and furthermore seems to be a good approximation to the finite-sized cylinder configurations considered previously. In this limit, the cylindrical ring is replaced by a cylindrical capsule of homogeneous material with uniaxial conductivity along the z axis: $\varepsilon(i\xi) = \mathrm{diag}(1,1,\infty)$. The capsule has a height
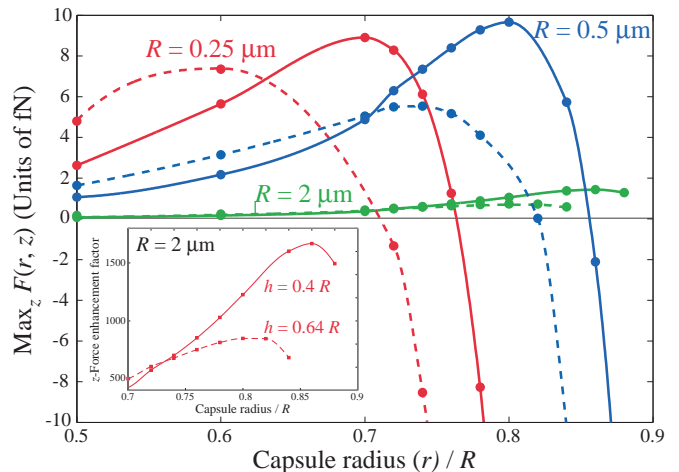

FIG. 5: Forces (maximized over z) for a thick cylindrical capsule composed of uniaxial conductor (Fig. 1, Bottom Right). In contrast to previous figures, here the plate thickness is fixed to $T = 20$ nm and the hole radius R is varied to three different values. For each R, the force is computed, as a function of capsule radius r, for capsule heights $h = 0.5R$ (solid lines) and $h = 0.64R$ (dashed lines). *Inset*: z-force enhancement factors as a function for both values of h for $R = 2\,\mu$m, which approximates a thin plate. The maximum force is approximately 10 fN.

h, outer radius r, and (for generality) inner radius r'; see Fig. 1 (d). Although we cannot simulate anisotropic materials with our boundary-element method, they can easily be treated with FDTD [21, 22]. This has the advantage that finite-thickness plates can be incorporated with no additional computational cost, and we can also exploit the cylindrical symmetry of the configuration to make the problem two-dimensional. In general the inner radius r' can be non-zero. However, we examined the difference in the force on a capsule as the inner radius r' is varied, and it turned out that this has almost no effect (less than 1%) on the force - the inner conducting material is almost, if not entirely, screened from the field of the plate. Therefore, without loss of generality in the following we set $r' = 0$ and consider solid cylinders only.

In the previous sections, we argued that the enhancement of Casimir repulsion in between the point dipole and PFA regimes is due to two effects - the increased size of the center object, and the increase in the fringing fields of the plate. We did this by separately examining each effect in turn. We are now in a position to examine the full combination of these effects, primarily to obtain an approximate upper bound on the possible strength of the repulsive effect assuming a fixed plate thickness T. To preserve contact with our previous work Ref. 1, in this section we fix our units so that $T = 20$ nm in all cases. From the results of previous sections, maximizing the repulsion over the remaining parameters (hole radius R, capsule radius r, capsule height h–here it is understood that we have already maximized over vertical displacement $z > 0$) will yield a finite peak repulsion. To simply

the presentation, we will write both h and r in units of the hole width R, so that only the radios h/R and r/R are relevant. Then for fixed h/R and r/R, as R is varied (keeping $T = 20\,\text{nm}$ always) we expect the force to scale as R^{-2} for $R \gg T$; as R decreases further, we expect the effect of $T > 0$ to overwhelm the R^{-2} scaling at some point, leaving an optimal value of R for each h/R and r/R. From the results of the previous section, we expect that examining both $h/R = 0.4$ and $h/R = 0.64$ will give a good estimate for the maximum force enhancement. For these two values, we consider three values of R, such that $T/R = 0.0025, 0.01$, and 0.02 (corresponding to $R = 2\,\mu\text{m}, 0.5\,\mu\text{m}, 0.25\,\mu\text{m}$, respectively). In Fig. 5 we plot the force for these six configurations as a function of capsule radius r. The case $R = 2\,\mu\text{m}$ is nearly indistinguishable from the thin plate case. To make contact with the results presented in previous sections, we plot the enhancement factor in the force for this case in the inset of Fig. 5. For $h/R = 0.64$, we get an enhancement similar to the previous section with multiple cylinders, while for $h/R = 0.4$ this factor is ~ 1600. Of course we know from previous results that this value can be made arbitrarily large; if we are to fix the plate thickness, we should consider instead the absolute magnitude of the repulsive force. When this is done, we see that going from $R = 2\,\mu\text{m}$ to $R = 0.5\,\mu\text{m}$ yields a further enhancement factor of 6, whereas for the $T = 0$ case it should be 16. When R is further decreased we see a decrease in the force for $h/R = 0.5$, and only a slight increase for $h/R = 0.64$. Further decreases in R (not shown) lead to a decrease in the force for both h. We see that although the enhancement factor for $R = 2\,\mu\text{m}$ is much larger for $h/R = 0.4$ than $h/R = 0.64$, the actual peak magnitudes for the forces are fairly similar for both values of h, and peak at approximately $10\,\text{fN}$. This is to be contrasted with the peak repulsive force found in Ref. 1, which was approximately $10\,\text{aN}$, and gives our quoted enhancement factor of $\sim 10^3$.

Additionally, we can use the uniaxial capsule configuration to examine the importance of our assumption of perfect conductors. Replacing the conducting plate with gold (plasma frequency $1.37 \times 10^{16}\,\text{rad/s}$) and the capsule with a material that has permittivity $\varepsilon(\omega) = \text{diag}(1, 1, \varepsilon_{\text{gold}}(\omega))$, we find that the peak repulsive force for $R = 2\,\mu\text{m}$ is reduced by 50%, but that for $R = 500\,\text{nm}$ it is only reduced by 20%, while for $R = 250\,\text{nm}$ it is *increased* by 10%. The increase in the repulsive force for smaller R can be understood from the fact (mentioned in [1]) that the attractive forces from finite-thickness plates come from high-ω components, which are cutoff by the plasma frequency in the gold permittivity. Therefore, using gold actually helps to attenuate some of the attractive effects introduced by using finite-thickness plates,

and implies that our force bounds remain valid for imperfect conductors. Finally, we examined the effect of introducing a long dielectric column attached to the capsule (this would serve as both an anchor for the capsule and a means of detecting the force on it). We find that a column made of silica (modeled as constant permittivity $\varepsilon = 2.25$) and of half the width of the capsule does not significantly modify the repulsive force. However, taking the column width equal to the capsule width reduces the peak repulsive force by a factor of 10.

IV. CONCLUSIONS

We have shown that Casimir repulsion is not limited to the small-particle dipole-interaction regime of our previous paper, and can in fact be considerably enhanced by considering interactions between macroscopic materials with highly anisotropic microstructures. As a practical matter, severe challenges remain in experimental realization of Casimir repulsion via this particular geometry. For an individual capsule with realistic conductivity, the force is only $10\,\text{fN}$, which, while 1000 times larger than the result of our previous paper, is still below the detection threshold of atomic force microscopy [24]. If this hole/capsule geometry were arranged in a periodic array with period twice the hole diameter (our numerical calculations indicate that this is sufficient to prevent interactions across holes), the repulsive pressure would be approximately $2\,\text{mPa}$ for $R = 500\,\mu\text{m}$, comparable to the attractive force between metal plates at $900\,\text{nm}$ separation, but the fabrication and alignment of such a structure appears extremely difficult. As a more general point, however, we believe that one route to obtaining a number of exotic Casimir effects would be to exploit effective uniaxial conductors formed by, e.g., vertical arrays of nanowires [25]. Even if the repulsive regime cannot be achieved, our results suggest that significant modifications to the Casimir force may result. Furthermore, other work has shown that additional exotic effects can be achieved by anisotropic patterning, such as orientation induced force transitions and torques [10], and anisotropic effects in many other geometries remain to be explored both theoretically and experimentally.

Near the completion of this work, a related paper [26] appeared which also examines (via analytical calculations) Casimir repulsion in geometries beyond the thin-plate/dipole regime, finding for example that repulsion persists when the plate has a wedge-like perpendicular profile as opposed to a thin line segment as considered here.

[1] M. Levin, A. P. McCauley, A. W. Rodriguez, M. T. Homer Reid, and S. G. Johnson, Phys. Rev. Lett. **105**, 090403 (2010).

[2] K. A. Milton, *The Casimir Effect: Physical Manifestations of Zero-Point Energy* (Singapore: World Scientific, 2001).

[3] A. W. Rodriguez, F. Capasso, and S. G. Johnson, Nature Phot. **5**, 211 (2011).

[4] B. V. Derjaguin, Kolloid Z. **69**, 155 (1934).

[5] S. J. van Enk, Phys. Rev. A **52**, 2569 (1995).

[6] C.-G. Shao, A.-H. Tong, and J. Luo, Phys. Rev. A **72**, 022102 (2005).

[7] J. N. Munday, D. Iannuzzi, Y. Barash, and F. Capasso, Phys. Rev. A **71**, 042102 (2005).

[8] O. Kenneth and S. Nussinov, Phys. Rev. D **63**, 121701(R) (2001).

[9] R. B. Rodrigues, P. A. Maia Neto, A. Lambrecht, and S. Reynaud, Europhys. Lett. **75**, 822 (2006).

[10] A. P. McCauley, F. S. S. Rosa, A. W. Rodriguez, J. D. Joannopoulos, D. A. R. Dalvit, and S. G. Johnson, Phys. Rev. A, *In Press* (2011).

[11] T. Emig, A. Hanke, R. Golestanian, and M. Kardar, Phys. Rev. A **67**, 022114 (2003).

[12] T. Emig, Phys. Rev. Lett. **98**, 160801 (2007).

[13] P. A. Maia Neto, A. Lambrecht, and S. Reynaud, Phys. Rev. A **78**, 012115 (2008).

[14] A. Lambrecht and V. N. Marachevsky, Phys. Rev. Lett. **101**, 160403 (2008).

[15] H.-C. Chiu, G. L. Klimchitskaya, V. N. Marachevsky, V. M. Mostepanenko, and U. Mohideen, Phys. Rev. B **81**, 115417 (2010).

[16] U. Leonhardt and T. G. Philbin, New J. Phys. **9**, 254 (2007).

[17] M. B. Romanowsky and F. Capasso, Phys. Rev. A **78**, 042110 (2008).

[18] F. S. S. Rosa, J. Phys. Conf. Ser. **161**, 012039 (2009).

[19] R. Zhao, J. Zhou, T. Koschny, E. N. Economou, and C. M. Soukoulis, Phys. Rev. Lett. **103**, 103602 (2009).

[20] M. T. Homer Reid, A. W. Rodriguez, J. White, and S. G. Johnson, Phys. Rev. Lett. **103**, 040401 (2009).

[21] A. W. Rodriguez, A. P. McCauley, J. D. Joannopoulos, and S. G. Johnson, Phys. Rev. A **80**, 012115 (2009).

[22] A. P. McCauley, A. W. Rodriguez, J. D. Joannopoulos, and S. G. Johnson, Phys. Rev. A **81**, 012119 (2010).

[23] S. J. Rahi, M. Kardar, and T. Emig, Phys. Rev. Lett. **105**, 070404 (2010).

[24] W. A. Goddard, D. Brenner, S. E. Lyshevski, and G. J. Iafrate, eds. (CRC Press, Boca Raton, FL, 2007), 2nd ed.

[25] C. Thelander, P. Agarwal, S. Brongersma, J. Eymery, L. F. Feiner, A. Forchel, M. Scheffler, W. Reiss, B. J. Ohlsson, U. Goesele, et al., Mat. Today **9**, 28 (2006).

[26] K. A. Milton, E. K. Abalo, P. Parashar, N. Pourtolami, I. Brevik, and S. A. Ellingsen, arXiv:hep-th/1103.4386 (2011).

[27] Formally, we must take the perfectly conducting limit before the $T \to 0$ limit